Highly-parallel, microfluidics-based force spectroscopy on single motor proteins

Marta Urbanska[1,†], Annemarie Lüdecke[1,*], Wilhelm J. Walter[1,2], Antoine M. van Oijen[3,4], Karl E. Duderstadt[3,5,6], Stefan Diez[1,7,8]

[1]B CUBE - Center for Molecular Bioengineering, Technische Universität Dresden, 01069 Dresden, Germany

[2]Biozentrum Klein Flottbek, Universität Hamburg, 22609 Hamburg, Germany

[3]Zernike Institute for Advanced Materials, University of Groningen, NL-9700 AE, Groningen, Netherlands

[4]Centre for Medical and Molecular Bioscience, Illawarra Health and Medical Research Institute and University of Wollongong, Wollongong, 2522 New South Wales, Australia

[5]Structure and Dynamics of Molecular Machines, Max Planck Institute of Biochemistry, 82152 Martinsried, Germany

[6]Physics Department, Technische Universität München, 85748 Garching, Germany

[7]Cluster of Excellence Physics of Life, Technische Universität Dresden, 01062 Dresden, Germany.

[8]Max Planck Institute of Molecular Cell Biology and Genetics, 01307 Dresden, Germany

†present address: Max Planck Institute for the Science of Light & Max-Planck-Zentrum für Physik und Medizin, 91058 Erlangen, Germany

*present address: NanoTemper Technologies GmbH, Flößergasse 4, 81369 München, Germany

Correspondence and requests for materials should be addressed to K.E.D. (email: duderstadt@biochem.mpg.de) and S.D. (email: stefan.diez@tu-dresden.de).

Abstract

Optical trapping experiments have provided crucial insight into the operation of molecular motors. However, these experiments are mostly limited to one measurement at a time. Here, we describe an alternative, highly-parallel, microfluidics-based method that allows for rapid data collection. We applied tunable hydrodynamic forces to stepping kinesin-1 motors via DNA-tethered beads and utilized a large field-of-view to simultaneously track the velocities, run lengths and interaction times of hundreds of individual kinesin-1 molecules under varying resisting and assisting loads. Importantly, the 16-µm long DNA tethers between the motors and the beads significantly reduced the vertical component of the applied force. Consequently, forces were predominantly exerted in the direction of motor movement, rather than away from the microtubule surface as unavoidable in conventional optical tweezers experiments. Our approach is readily applicable to other motors and constitutes a new methodology for parallelized single-molecule force studies.

Keywords: Single-Molecule Force Spectroscopy, Molecular Motors

The application and detection of forces using single-molecule manipulation methods has provided major advances in our understanding of the operating principles of mechanoenzymes[1–4]. Optical and magnetic tweezers as well as atomic force microscopy are now being routinely used to study protein folding pathways, receptor-ligand interactions, DNA mechanics and the activity of molecular motors. While all of these experimental approaches offer excellent spatiotemporal resolution and force accuracy—with different force spectra and displacement ranges covered—none of them provides high experimental throughput as conventionally only one molecule is studied at a time. This limitation constitutes one of the major bottlenecks in current single-molecule force measurements[4,5], where the derivation of statistically significant results from stochastic single-molecule footprints is desired in reasonable time frames. Consequently, continuous efforts are being made to surpass this limitation in the field of optical[6–8] and magnetic trapping[9–11] as well as in atomic force microscopy—regarding both instrumental automation[12] and sample preparation[13]. Alongside, a number of novel solutions for multiplexed force manipulation, such as centrifuge force microscopy[14,15] and acoustic force spectroscopy[16], are being introduced. So far, the use of these novel methods has been demonstrated for the studies of DNA mechanics, DNA-protein binding and protein-protein binding but not for cytoskeletal motor proteins. While their use to study DNA motors is conceivable, they may require modifications to become applicable for studies on cytoskeletal motors because of the vertical character of the applied force.

One so far largely unexploited way to apply calibrated forces onto individual molecules is hydrodynamic flow. In a microfluidic environment, laminar flow can be used to exert Stokes drag on micrometer-sized beads that act as force handles when linked to surface-attached biomolecular mechanosystems. The magnitude of the drag force is determined by the diameter of the beads and the velocity of the flow. The latter can be kept constant over large regions in a microfluidic chamber. The response of the molecular system under investigation can then be deduced by tracking the positions of multiple beads simultaneously using an optical microscope. Hence, the number of constant-force experiments performed at a time is in principle limited only by the size of the imaged area and the surface density of the bead-coupled mechanosystems. Low-throughput experiments using hydrodynamic flow have previously been performed to study single-molecule forces in protein unfolding[17], to measure rupture forces of streptavidin-biotin bonds[18], to investigate the confining potential felt by individual membrane-embedded receptors[19], and, in the context of cytoskeletal motors, to measure the adhesion forces of beads covered with multiple kinesin-1 motors to microtubules[20]. Moreover, high-throughput experiments using hydrodynamic flow have been performed to study DNA mechanics and DNA-protein interactions. In particular, highly-parallel measurements to monitor the enzymatic activity of DNA exonucleases[21], DNA and

RNA polymerases[22–24], or topoisomerases[25] have been demonstrated on flow-stretched DNA, with force control down to 0.1 pN.

Here, we demonstrate the application of hydrodynamic forces to investigate the translocation of cytoskeletal motors under load in a highly parallel manner. In particular, we use paramagnetic beads attached to individual kinesin-1 motors via 16-μm long DNA linkers as force handles and utilized a large field-of-view microscope to characterize the velocities, run lengths and interaction times of hundreds of motors stepping under a series of in situ calibrated force conditions. Leveraging the large spatially homogenous force field generated by hydrodynamic flow and the use of a specialized telecentric lens capturing a field-of-view of several millimeters in size, we were able to optically track hundreds of individual molecules in a single experiment, amounting to a total of 2500 events in eight experiments. Consistent with previous low-throughput measurements with optical tweezers, our data shows that the velocity of kinesin-1 motors gradually decreased under increasing load by up to 60% for resisting loads of about 3 pN, and by up to 32% for assisting loads of the same magnitude. Due to the molecular geometry of our assay, we were able to directly measure the motility parameters of kinesin-1 in the absence of significant vertical forces (i.e. away from the microtubule surface), which had previously been only accessible by theoretical calculations. Our high-throughput method does not require expensive equipment and can be easily adapted to other biomolecular mechanosystems.

To assemble the molecular system for the velocity measurements of individual kinesin-1 motors stepping along microtubules under load, we sequentially attached specially designed molecular components to the surface of a flow cell (Fig. 1a and Methods). First, GMPCPP-stabilized microtubules were immobilized on the flow cell surface via anti-β-tubulin antibodies. Next, truncated, SNAP-tagged kinesin-1 motors were covalently coupled to 16.2-μm-long double-stranded DNA (dsDNA) linkers based on lambda phage DNA (λ-DNA) with functionalized ends. The kinesin-DNA complexes were then introduced to the flow cell and attached to the microtubules in presence of 100 μM AMPPNP. Finally, 1-μm sized superparamagnetic beads coated with anti-digoxigenin antibodies were attached to the free ends of the DNA linkers. The AMPPNP kept the kinesin-1 motors at fixed positions on the microtubules until the beginning of the measurement which was initiated by the addition of 10 mM ATP (Supplementary Fig. 1). Evaluation of the extreme positions of the beads during flow reversal showed that the length of most tethers corresponds to the full length single λ-DNA (Supplementary Fig. 2), indicating prevalence of full-length molecules with single attachment sites.

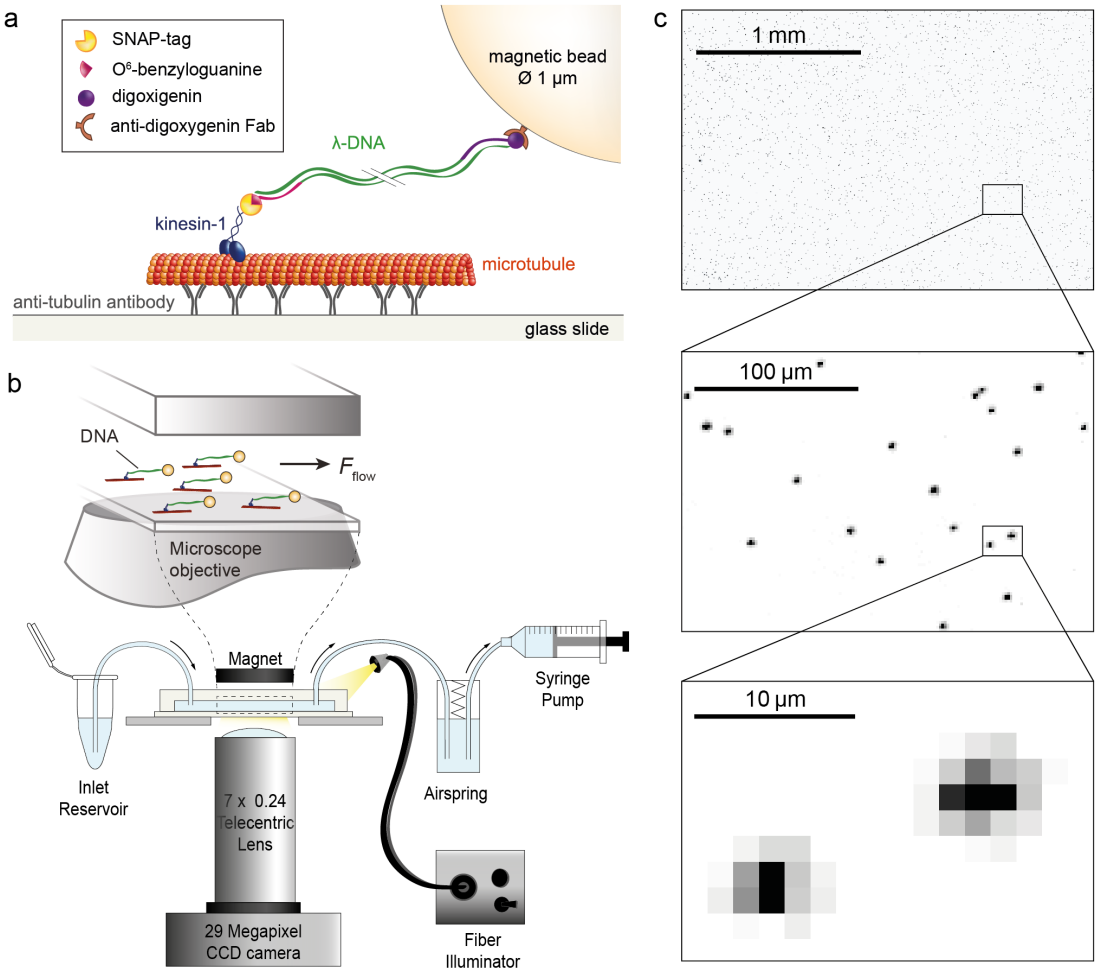

Figure 1| Kinesin-1 microfluidics-based force assay. (a) Molecular details of attaching a 1-µm sized paramagnetic bead to an individual kinesin-1 motor via a long, double-stranded DNA linker. (b) Schematic overview of the experimental setup. Inset presents a side view of the interior of the flow cell (not to scale). The direction of applied force is indicated by the arrow. (c) Dark-field microscopy images of multiple magnetic beads (up to 30,000 beads per field-of-view) tethered to individual kinesin-1 motors. The top panel represents only 23 % of the full field-of-view.

To perform the microfluidics-based force assay, the flow cell was mounted on a custom-made inverted microscope, which constituted the heart of the experimental setup (Fig. 1b). A syringe pump, operated in withdrawal mode, was used to apply a constant hydrodynamic flow throughout the experiment. An air spring was introduced between the flow cell outlet and the pump in order to damp any flow irregularities. To minimize interactions of the tethered beads with the surface, a magnet installed on the top of the flow cell provided a miniscule force of ~0.1 pN to lift the paramagnetic beads off the surface. To observe the bead positions, the flow cell was illuminated from the side with high-intensity white light from a fiber illuminator. The light scattered by the beads was collected through a telecentric lens and projected onto a CCD camera. Due to the large scattering cross-section of the beads it was possible to implement a low-magnification objective to maximize the field-of-view without substantial loss in accuracy when determining the bead positions. Moreover, the high quality of the telecentric lens kept the image undistorted towards the

edges and, together with the 29 Megapixel camera sensor, provided for imaging of an 18 mm^2 large region. Within one field-of-view it was possible to image up to 30,000 beads (Fig. 1c) and each of them could be tracked with a precision of 32 nm (see Supplementary Methods).

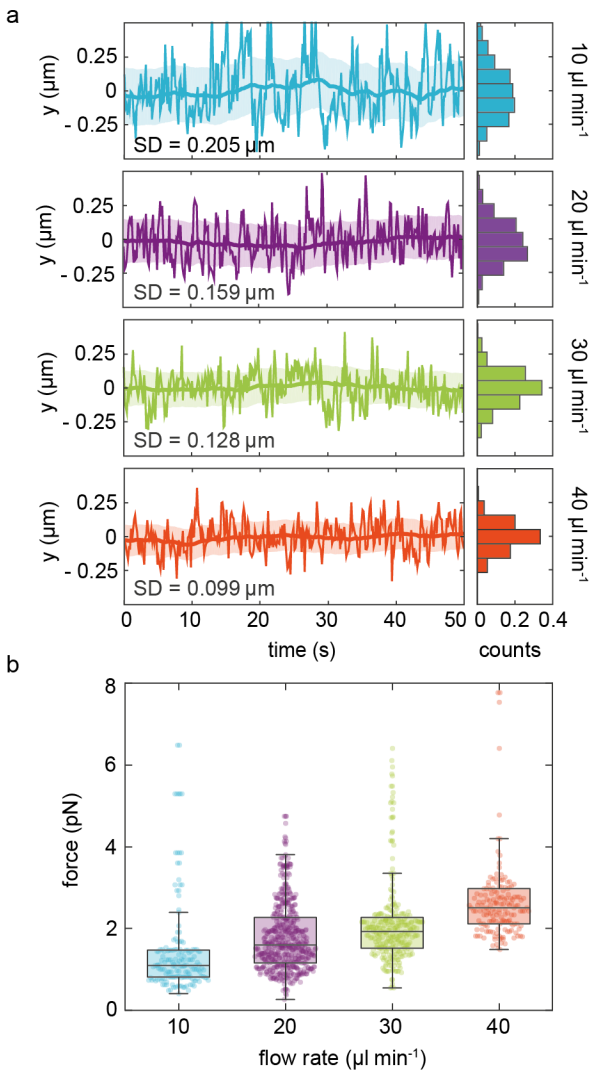

Figure 2| Fluctuation-based in situ force calibration. (a) Bead fluctuations in the direction *y* transverse to the flow over time for flow rates of 10, 20, 30 and 40 µl min^{-1}. Histograms on the right-hand side present relative occurrences of *y* positions. (b) Distributions of estimated forces for different flow rates. Boxes extend from 25th to 75th percentiles, with a line at the median. Whiskers span 1.5× interquartile range. Colored dots represent individual beads (n = 162, 553, 285, 169).

As routinely used in the field of magnetic tweezers, we used the fluctuations of the tethered beads in the direction transverse to the flow for an in situ calibration of the acting forces[26]. By relating the energy of a Hookean spring to the equipartition theorem the following equation is obtained:

$$\langle \delta y^2 \rangle = \frac{k_B T l}{F}. \qquad (1)$$

The mean-square displacement of a bead in the transverse direction $\langle \delta y^2 \rangle$, together with the length of the tether l, temperature T and Boltzmann constant k_B are sufficient to determine the force F pulling on the molecule. To enable precise determination of the tether extension for each molecule,

we coupled the force-extension relation for dsDNA[27] with equation (1) and solved the set of these two equations numerically to obtain both tether extension and force magnitude for each molecule individually (see Supplementary Methods for details, including a correction for motion blurring caused by the finite camera integration time).

The measured magnitude of the fluctuations of individual beads decreased with increasing flow rate (Fig. 2a). Using the trajectories from all beads which exhibited unidirectional movement after the addition of ATP, we determined a characteristic force for each experiment. Figure 2b presents the force distributions for exemplary experiments performed at flow rates of 10, 20, 30 and 40 $\mu l\ min^{-1}$. The median forces in the presented experiments were 1.1, 1.6, 1.9 and 2.5 pN, respectively.

Next, we looked at the motility of individual kinesin-1 motors under resisting and assisting loads. After AMPPNP had been washed out by ATP-containing buffer the motors started to translocate (Supplementary Fig. 1), predominantly along the flow axis as the majority of the microtubules were aligned by the flow (Supplementary Fig. 3). We discriminated between different stepping directions by looking at the bead displacement in the *x-y* plane. Exemplary trajectories of kinesin-1 motors moving against the flow (i.e. experiencing a resisting load) and with the flow (i.e. experiencing an assisting load) are presented in Figures 3a and 3b, respectively.

Although the microtubule axes were mostly aligned with the flow direction, their polarities (i.e. the positions of their plus and minus ends) were arbitrary. Therefore, we were able to investigate the motility of individual plus-end directed kinesin-1 motors under resisting and assisting loads of the same magnitude simultaneously. Velocity histograms from a single experiment with 444 motility events against the flow and 476 motility events with the flow are presented in Figures 3c and 3d. Under a median load of 1.6 pN in the presented experiment, the kinesin-1 motors stepped with mean velocities of $0.410 \pm 0.161\ \mu m\ s^{-1}$ against the flow and $0.557 \pm 0.296\ \mu m\ s^{-1}$ with the flow.

By varying the flow rates, we applied loads of different magnitudes and constructed a force-velocity curve for kinesin-1 (Fig. 4a). Since the distribution of forces acting on the molecules under a given flow rate is considerably broad (Fig. 2b), we assigned force loads to each stepping event individually and compared velocities for the data grouped according to the estimated values into 0.3-pN wide bins. We observe that with increasing resisting load the stepping velocity of kinesin-1 progressively decreased. It reached a mean value of $0.532 \pm 0.200\ \mu m\ s^{-1}$ (mean ± SD) for the lowest load bin (0.9 ± 0.15 pN) and $0.266 \pm 0.123\ \mu m\ s^{-1}$ for the highest load bin (3 ± 0.15 pN). Under conditions of assisting load, we found the highest velocity of $0.686 \pm 0.290\ \mu m\ s^{-1}$ for the lowest load bin. With increasing assisting load, the kinesin-1 stepping velocity slightly decreased and reached a mean value of $0.441 \pm 0.264\ \mu m\ s^{-1}$ for the highest load bin. The force-velocity curve obtained for kinesin-1 in our study follows qualitatively[26] and even quantitatively[27] earlier data from optical

tweezers measurements for resisting loads (Fig. 4d). We note, that contrary to the data reported in Ref. [28,29] but consistent with trend of the data reported in Ref. [27] the velocity observed in our experiments showed a marked decrease under increasing assisting loads.

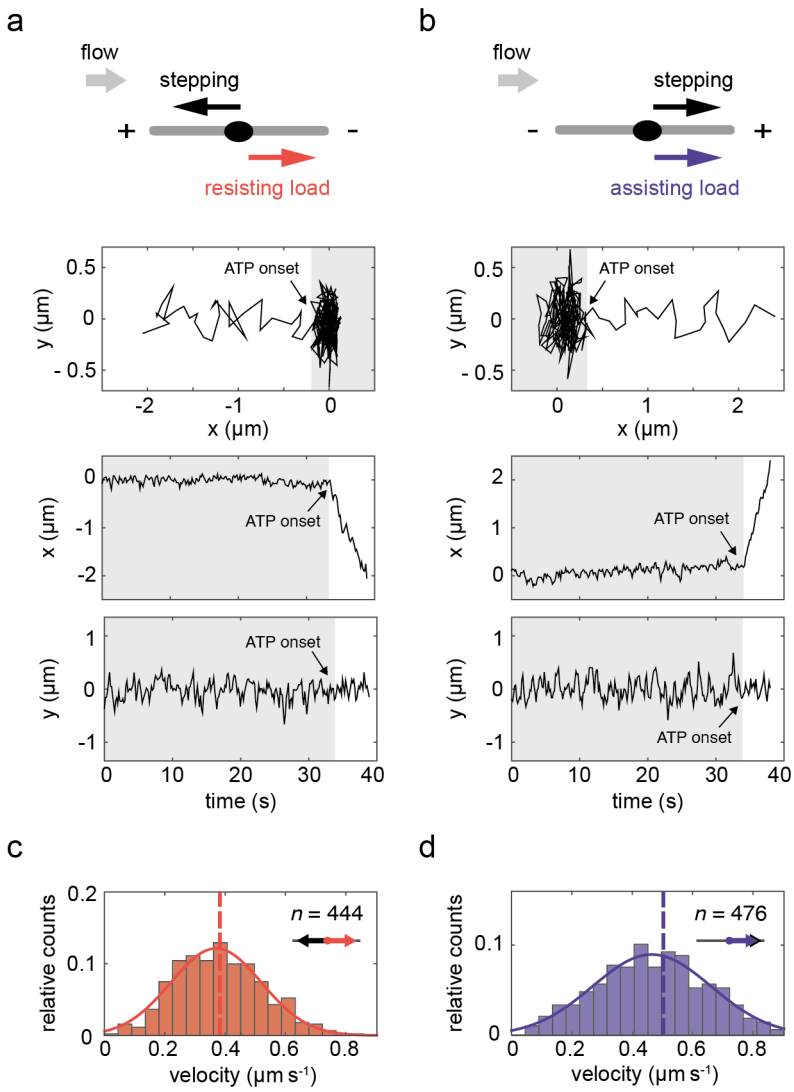

Figure 3 | Single-molecule motility events under resisting and assisting load. (a) Setup and exemplary trajectory of a motor stepping against the flow (towards decreasing *x*-position, corresponding to a resisting load). The plots from top to bottom present: the position of the bead in a 2D plane over 40 seconds before detachment, the *x*-position over time and *y*-position over time. The gray-shaded areas correspond to the period before ATP onset, i.e. the time when the motors were still arrested in the presence of AMPPNP. (b) Analogous setup and exemplary trajectory of a motor stepping with the flow (towards increasing *x*-position, corresponding to an assisting load). (c) Velocity histogram of 444 stepping events under resisting load. (d) Velocity histogram of 476 stepping events under assisting load. In c and d, overlays of Gaussian fits are presented and vertical dashed lines represent mean velocity values.

Apart from velocity, we were also able to readily evaluate the run lengths and interaction times of individual kinesin-1 motors under the different loads (Fig. 4b–c). To account for under-representation of very short stepping events, we estimated these two parameters using least-squares fitting of the cumulative distribution function with free cut-off parameters[30]. The measured run lengths appeared fairly constant at about 0.62 μm for loads between -2.7 pN and 2.1 pN (Fig. 4b). For assisting load larger than 2.7 pN and resisting loads larger than 2.1 pN the run lengths decreased. This is in contrast to observations made with optical tweezers, where the measured run lengths decreased already drastically for moderate loads, e.g. showing a three-fold decrease at 2 pN resisting load[31]. We hypothesize that it is the high vertical force contribution that causes the premature detachment of motors in these earlier measurements. The mean run-length value of 0.62 μm observed at low loads in our experiments, corresponds well to the previously reported values of ~0.68 μm for unloaded motors[30].

The measured interaction times appeared fairly constant at about 0.77 s for all applied assisting loads. For resisting loads the interaction times appeared fairly constant at about 1.28 s up to 2.7 pN before decreasing above that load. The overall higher interaction times observed under resisting loads, as compared to assisting loads, suggest that kinesin-1 exhibits a higher detachment rate under assisting loads. This is in agreement with the higher unbinding force observed for kinesin-1 under resisting load as compared to assisting load[32] and with the theoretical prediction that horizontal forces alone, as predominantly present in our setup, decelerate motor detachment[33,34]. The mean interaction times obtained for both assisting and resisting loads, correspond well to the interaction time of 0.95 s under unloaded conditions reported previously for the same kinesin-1 construct at room temperature[30]. The good agreements of both run length and interaction time with previously reported and predicted values for single kinesin-1 motors ascertains that we evaluated the stepping of single motors.

The marked differences in kinesin-1 motility parameters between our assay and the optical tweezers experiments highlight the importance of the load geometry in the single-molecule force measurements. The different loading scenarios may reflect the physiological transport of cargos differing in size or shape inside the cell, or differently positioned motors in multi-motor assemblies present in vivo.

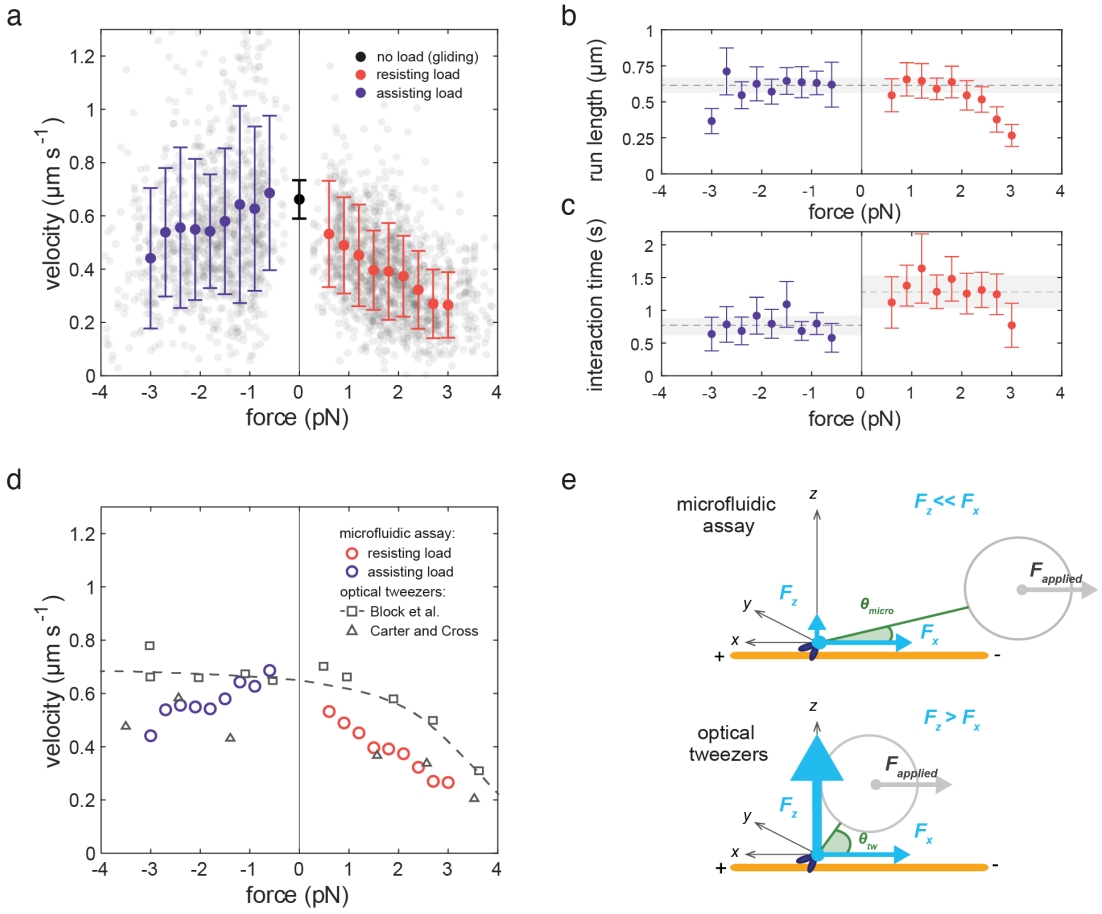

Figure 4 | Force-dependence of motility parameters for kinesin-1 as probed by the microfluidic assay. (a) Stepping velocity of kinesin-1 observed under assisting (violet dots) and resisting (red dots) loads of different magnitudes. Plotted values represent means ± SD of velocity data contained within 0.3-pN force bin (n = 52–213 per bin). Gray scatter represents individual events used for binning (n = 2484). The black dot represents the velocity of the kinesin-1 motor used in this study under no load condition as evaluated by gliding assays (mean ± SD, see Supplementary Fig. 4). (b,c) Force dependence of run lengths and interaction times for events in (a), plotted values represent means ± 2×SD obtained from bootstrapping. As guides for the eye, means of bins -2.7 to 2.1 pN for run length, and mean of all assisting as well as all resisting load bins for interaction time, are indicated with the dashed gray line. Shaded areas represent SD. (d) Overlay of force-velocity data from our study (violet and red open circles) with data obtained in optical tweezers' studies by Block et al.[28] (open squares, mean velocities with dashed curve showing the fit of a five-step model) and by Carter and Cross[29] (open triangles, mean velocities). (e) Comparison of experimental geometries in the microfluidic assay presented in this study (upper scheme) and in a typical optical tweezers experiment (lower scheme). θ - inclination angle between the microtubule and the tether in the case of the microfluidic setup (θ_{micro}) and a typical optical tweezer configuration (θ_{tw}); $F_{applied}$ – force applied on the bead; F_z – vectorial component of the force pointing in the z direction (vertical force); F_x - vectorial component of the force pointing in the x direction (horizontal force).

Our hydrodynamic force assay not only enables parallelization of the measurements on cytoskeletal motors, but also provides an alternative geometry of force application compared to existing methods. While optical traps—the method of choice for characterizing cytoskeletal motors—have been exploited to study the application of forward, backward[29,31,35], and sideward loads[28,36] on stepping kinesins using a variety of geometries[37,38], they generally suffer from a poor control over vertically applied forces, which may bias the measurements performed[39–42]. Although the force is applied horizontally onto the bead in a conventional optical trap experiment, the molecule under investigation is experiencing a vertical load which, in fact, can surpass the applied horizontal force

in magnitude[39]. Such substantial vertical load is pulling the motor away from the filament and can influence its stepping velocity and detachment rate[39,42]. In our approach, the introduction of a spacer between the motor and the bead reduces the vertical force component to less than 15% of the applied force (see Fig. 4e and Supplementary Table 1), thus applying forces more stringently in the direction of motor movement than in optical tweezers experiments. Optimal performance of our method is achieved at intermediate forces. At very low forces (< 0.5 pN) the bead fluctuations limit the accuracy of the velocity measurements. At high forces, in turn, the observation time is limited due to the decreased processivity of the motor. However, the latter is specific to single kinesin-1 motors, exhibiting a force-dependent run length[31], and will likely not be an issue for other mechanosystems, such as dynein[43] or multi-motor transport systems[44].

An additional asset of our method is the possibility to study the motor velocity in an angle-resolved manner (see Supplementary Fig. 5). Depending on the alignment of the microtubules with respect to the flow direction, some motors will step not directly against or with the direction of applied force. In this study, the microtubules were aligned with the long flow cell axis to maximize the number of events stepping parallel to the force direction (Supplementary Fig. 3), however, the orientation of the microtubules can be randomized by applying a perpendicular or turbulent flow while introducing microtubules to the flow cell. The straightforward in situ force calibration and the flexibility of the assay geometry design due to adjustable DNA tether length and possibility to manipulate the bead height by changing the magnetic force, further enhance the appeal of the presented method. Finally, we note that our approach can be implemented using any standard wide-field microscope at low cost.

Single-molecule manipulation techniques have shed light on the functioning principles of many molecular machines in the cell. Yet, their widespread applicability and utilization for single-molecule screening purposes is limited by the lack of robust high-throughput technologies. Our versatile, massively multiplexed microfluidic assay for the application of forces to molecular mechanosystems, such as stepping cytoskeletal motors and motor complexes, presents a leap towards wider usage of single-molecule approaches. We envision a broad implementation of the assay in fundamental research of biological systems as well as in medical diagnostics applications, where rapid acquisition of population-wide data is of key importance.

Author Contributions

S.D., A.M.O. and W.J.W. conceived the project. M.U., with support of A.L., W.J.W. and K.E.D. performed the experiments. W.J.W. cloned and expressed the SNAP-tagged kinesin-1 protein. M.U. and K.E.D. wrote the analysis software. M.U. analyzed the data, prepared figures and wrote the original version of the manuscript. All authors revised and edited the manuscript. S.D., K.E.D., A.M.O. and W.J.W. supervised the project. S.D. and K.E.D. acquired funding.

Acknowledgements

We thank Corina Bräuer and Cornelia Thodte for technical assistance, Felix Ruhnow and Erik Schäffer for fruitful discussions, Lucas Wittwer and Sebastian Aland for help with theoretical considerations, and Georg Krainer for helpful suggestions on the manuscript. We acknowledge financial support from the Dresden International Graduate School for Biomedicine and Bioengineering (DIGS-BB, stipend to A.L.), the German Excellence Initiative (TU Dresden Support-the-Best grant to S.D.), the Human Frontier Science Program (Long-term fellowship LT000180/2012-L to K.E.D.), and support from the Max Planck Society to K.E.D.

References

1. Bustamante, C., Macosko, J. C. & Wuite, G. J. Grabbing the cat by the tail: manipulating molecules one by one. *Nat. Rev. Mol. Cell Biol.* **1**, 130–6 (2000).

2. Clausen-Schaumann, H., Seitz, M., Krautbauer, R. & Gaub, H. E. Force spectroscopy with single bio-molecules. *Curr. Opin. Chem. Biol.* **4**, 524–530 (2000).

3. Neuman, K. C. & Nagy, A. Single-molecule force spectroscopy: optical tweezers, magnetic tweezers and atomic force microscopy. *Nat. Methods* **5**, 491–505 (2008).

4. de Souza, N. Pulling on single molecules. *Nat. Methods* **9**, 873–877 (2012).

5. Alsteens, D., Tay, S. & Müller, D. J. Toward high-throughput biomechanical phenotyping of single molecules. *Nat. Publ. Gr.* **12**, 45–46 (2015).

6. Emiliani, V., Sanvitto, D., Zahid, M., Gerbal, F. & Coppey-Moisan, M. Multi force optical tweezers to generate gradients of forces. *Opt. Express* **12**, 3906–3910 (2004).

7. Soltani, M. *et al.* Nanophotonic trapping for precise manipulation of biomolecular arrays. *Nat. Nanotechnol.* **9**, 448–52 (2014).

8. Tanaka, Y. & Wakida, S. Time-shared optical tweezers with a microlens array for dynamic microbead arrays. *Biomed. Opt. Express* **6**, 3670 (2015).

9. De Vlaminck, I. & Dekker, C. Recent Advances in Magnetic Tweezers. *Annu. Rev. Biophys.* **41**, 453–472 (2012).

10. Kriegel, F. *et al.* Probing the salt dependence of the torsional stiffness of DNA by multiplexed magnetic torque tweezers. *Nucleic Acids Res.* **45**, 5920–5929 (2017).

11. Santos, Á., Fili, N., Pearson, D. S., Hari-gupta, Y. & Christopher, P. High throughput mechanobiology: Force modulation of ensemble biochemical and cell-based assays. *bioRxiv* 10.1101/2020.05.05.065912 (2020) doi:10.1101/2020.05.05.065912.

12. JPK Instruments AG. Single molecule force spectroscopy with the ForceRobot® 300. http://usa.jpk.com/index.231.us.html.

13. Otten, M. *et al.* From genes to protein mechanics on a chip. *Nat. Methods* **11**, 1–7 (2014).

14. Halvorsen, K. & Wong, W. P. Massively parallel single-molecule manipulation using centrifugal force. *Biophys. J.* **98**, L53–L55 (2010).

15. Yang, D., Ward, A., Halvorsen, K. & Wong, W. P. Multiplexed single-molecule force spectroscopy using a centrifuge. *Nat. Commun.* **7**, 1–7 (2016).

16. Sitters, G. *et al.* Acoustic force spectroscopy. *Nat. Methods* **12**, 47–50 (2015).

17. Zocchi, G. Proteins unfold in steps. *Proc. Natl. Acad. Sci. U. S. A.* **94**, 10647–10651 (1997).

18. Zocchi, G. Force measurements on single molecular contacts through evanescent wave microscopy. *Biophys. J.* **81**, 2946–2953 (2001).

19. Türkcan, S., Richly, M. U., Bouzigues, C. I., Allain, J.-M. & Alexandrou, A. Receptor displacement in the cell membrane by hydrodynamic force amplification through nanoparticles. *Biophys. J.* **105**, 116–26 (2013).

20. Yokokawa, R., Sakai, Y., Okonogi, A., Kanno, I. & Kotera, H. Measuring the force of adhesion between multiple kinesins and a microtubule using the fluid force produced by microfluidic flow. *Microfluid. Nanofluidics* **11**, 519–527 (2011).

21. Oijen, A. M. Van, Blainey, P. C. & Crampton, D. J. Single-Molecule Kinetics of Exonuclease Reveal Base Dependence. *Science (80-.).* 1235–1238 (2003).

22. Lee, J. B. *et al.* DNA primase acts as a molecular brake in DNA replication. *Nature* **439**, 621–624 (2006).

23. Tanner, N. a *et al.* Real-time single-molecule observation of rolling-circle DNA replication. *Nucleic Acids Res.* **37**, e27 (2009).

24. Duderstadt, K. E. *et al.* Simultaneous Real-Time Imaging of Leading and Lagging Strand Synthesis Reveals the Coordination Dynamics of Single Replisomes. *Mol. Cell* **64**, 1035–1047 (2016).

25. Agarwal, R. & Duderstadt, K. Multiplex flow magnetic tweezers reveal rare enzymatic events with single molecule precision. *(accepted).*

26. Strick, T. R., Allemand, J. F., Bensimon, D. & Croquette, V. Behavior of supercoiled DNA. *Biophys. J.* **74**, 2016–28 (1998).

27. Bustamante, C., Marko, J. F., Siggia, E. D. & Smith, S. Entropic Elasticity of λ-Phage DNA. *Science (80-.).* **265**, 1599–1600 (1994).

28. Block, S. M., Asbury, C. L., Shaevitz, J. W. & Lang, M. J. Probing the kinesin reaction cycle with a 2D optical force clamp. *Proc. Natl. Acad. Sci. U. S. A.* **100**, 2351–6 (2003).

29. Carter, N. J. & Cross, R. a. Mechanics of the kinesin step. *Nature* **435**, 308–12 (2005).

30. Ruhnow, F., Kloβ, L. & Diez, S. Challenges in Estimating the Motility Parameters of Single Processive Motor Proteins. *Biophys. J.* **113**, 2433–2443 (2017).

31. Schnitzer, M. J., Visscher, K. & Block, S. M. Force production by single kinesin motors. *Nat. Cell Biol.* **2**, 718–23 (2000).

32. Uemura, S. *et al.* Kinesin-microtubule binding depends on both nucleotide state and loading

direction. *Proc. Natl. Acad. Sci.* **99**, 5977–5981 (2002).

33. Khataee, H. & Howard, J. Force Generated by Two Kinesin Motors Depends on the Load Direction and Intermolecular Coupling. *Phys. Rev. Lett.* **122**, 188101 (2019).

34. Khataee, H., Neufeld, Z. & Mahamdeh, M. Processivity of molecular motors under vectorial loads. *bioRxiv* 2020.04.13.039784 (2020) doi:10.1101/2020.04.13.039784.

35. Nishiyama, M., Higuchi, H. & Yanagida, T. Chemomechanical coupling of the forward and backward steps of single kinesin molecules. *Nat. Cell Biol.* **4**, 790–7 (2002).

36. Lang, M. J., Asbury, C. L., Shaevitz, J. W. & Block, S. M. An automated two-dimensional optical force clamp for single molecule studies. *Biophys. J.* **83**, 491–501 (2002).

37. Bugiel, M., Böhl, E. & Schäffer, E. The kinesin-8 Kip3 switches protofilaments in a sideward random walk asymmetrically biased by force. *Biophys. J.* **108**, 2019–2027 (2015).

38. Bugiel, M., Mitra, A., Girardo, S., Diez, S. & Schäffer, E. Measuring Microtubule Supertwist and Defects by 3D-Force-Clamp Tracking of Single Kinesin-1 Motors. *Nano Lett.* acs.nanolett.7b04971 (2018) doi:10.1021/acs.nanolett.7b04971.

39. Kim, Y. C. & Fisher, M. E. Vectorial loading of processive motor proteins: implementing a landscape picture. *J. Phys. Condens. Matter* **17**, S3821-38 (2005).

40. Kolomeisky, A. B. & Fisher, M. E. Molecular motors: a theorist's perspective. *Annu. Rev. Phys. Chem.* **58**, 675–95 (2007).

41. Fisher, M. E. & Kim, Y. C. Kinesin crouches to sprint but resists pushing. *Proc. Natl. Acad. Sci. U. S. A.* **102**, 16209–14 (2005).

42. Gittes, F., Meyhöfer, E., Baek, S. & Howard, J. Directional loading of the kinesin motor molecule as it buckles a microtubule. *Biophys. J.* **70**, 418–29 (1996).

43. Nicholas, M. P. *et al.* Cytoplasmic dynein regulates its attachment to microtubules via nucleotide state-switched mechanosensing at multiple AAA domains. *Proc. Natl. Acad. Sci.* **112**, 6371–6376 (2015).

44. Kunwar, A., Vershinin, M., Xu, J. & Gross, S. P. Stepping, Strain Gating, and an Unexpected Force-Velocity Curve for Multiple-Motor-Based Transport. *Curr. Biol.* **18**, 1173–1183 (2008).